Berkala Fisika *ISSN : 1410 – 9662*
Vol. 16, No. 3, Juli 2013, hal 95 - 102

OPTICAL AND MAGNETIC PROPERTIES OF TeO_2·ZnO·Li_2O GLASS SYSTEM CONTAINING NATURAL Fe_3O_4 PARTICLES

W. Widanarto[a], M. R. Sahar[b,*], S. K. Ghoshal[b], R. Arifin[b], M. S. Rohani[b]
[a]*Physics Study Program, Universitas Jenderal Soedirman, Jl. dr. Soeparno 61 Purwokerto 53123, Indonesia*
[b]*Department of Physics, Faculty of Science, Universiti Teknologi Malaysia, Johor Bahru, Skudai 81310, Malaysia*

Abstract

Natural Fe_3O_4 particles obtained by extracting and manual pulverizing natural iron sand, are doped in the TeO_2·ZnO·Li_2O glass system by melt quenching technique at 800 ℃. X-ray diffraction spectra confirms the presence of iron sand particles with the 33-146 nm diameters and the glassy structure.Vibrating sample magnetometer reveals the pulverized sand exhibits paramagnetic behaviour with magnetic susceptibility of 2.76 × 10^{-4} m^3 kg^{-1}. Incorporation of the particles in the glasses changes color, thermal stability and improve the glass formation ability through value of T_c–T_g. Ultraviolet–visible measurements show the optical energy band gap decreases by 1.58 eV. Meanwhile, the resonance amplitude of the electron spin resonance spectrum decreases due to the presence of Fe_3O_4 particles in reducing the unpaired electron spin. The synthesized glasses exhibit paramagnetic behavior.

Keywords: *Iron Sand, Ferrite oxide, Tellurite, Glass, Optical band gap, Magnetic property, ESR*

Introduction

Fe_3O_4 particles are ferrite oxide with an inverse cubic spinel structure. In the structure, an oxygen ion splits metallic ions. Broad distance between the metallic ions causes occurring an exchange between the metallic ions via the oxygen ion [1–3]. These compounds have unique electrical and magnetic properties due to electron transfer between Fe^{2+} and Fe^{3+} in tetrahedral and octahedral sites [4].

Natural iron sand are mostly in forms of magnetite (Fe_3O_4), hematite (α-Fe_2O_3) and maghemite (γ-Fe_2O_3). The magnetite is common ferrite oxides. Natural ferrite oxide particles can be obtained by extracting the sand [2]. The particles incorporated in oxide glass plays important role due to their magnetic, optical and electrical properties [5,6]. Futhermore, the transition metal ions will contribute multivalence states in the glass, which is possible to be applied as cathode material in litthium batteries [7].

Tellurium dioxide (TeO_2) is the most stable oxide of tellurium (Te), with a melting point of 733 °C [8]. The stability of tellurium oxides is one of the outstanding properties that makes researchers interested in crystalline solids and tellurite glasses. In addition, the nonlinear optical properties of these glasses are suitable for photonic applications such as optical modulators and memories [9,10]. Even though many investigations on tellurite glasses not many efforts are devoted towards the incorporation of natural Fe_3O_4 particles in these glasses. Therefore, in this work the particles are incorporated in tellurite glass using melt quenching technique and further characterized for structural, optical and magnetic properties.

Experimental

Preparation of ferrite oxide particles

Natural iron sand is taken from the coastal region and rinsed [2]. The obtained particles are manually pulverized for 1 h using mortar and pestle to reduce their size below 75 μm and to purify ferrite oxide from unexpected substances. Finally, a permanent magnet is used to ensure that the captured particles are only magnetic particles of ferrite oxide.

Preparation of glasses

Glass samples with chemical composition $70TeO_2{\cdot}15ZnO{\cdot}15Li_2O$ in mol% are synthesized by melt quenching technique. Bulk glasses in the glass system are prepared in 10 g batches using high purity chemicals i.e. tellurite dioxide (TeO_2 99+%: Acros), zinc oxide (ZnO 99.9%: Sigma Aldrich) and lithium carbonate (Li_2CO_3 99.99%: Sigma Aldrich). The chemicals are weighed using an electronic balance according to quantities of their analytical grade and mixed in a porcelain crucible. The natural ferrite oxide particles in weighs of 0.36 g are added in mixed chemicals. The chemicals contained crucible are pre-heated in an electrical furnace (Carbolite) at temperature of 300 °C for 20 min to evaporate water and CO from the chemicals due to water absorption during weighing and using Li_2CO_3. After that the crucible is moved to second furnace for melting process at temperature of 800 °C for 20 min. The melt is poured on pre-heated stainless steel plate and pressed by another pre-heated steel plate to form a glass in an other furnace. Immediately, the quenched melt is annealed at 300 °C for 3 h and naturally cooled down to the room temperature [2,3,11].

Characterizations

Low vacuum scanning electron microscopy (LVSEM – JSM 6360) and X–ray diffraction (XRD) are used to confirm surface morphology and compound of the pulverized iron sand particles. Sizes of the particles are estimated from XRD data using Debye–Scherrer's formula [12,13], meanwhile magnetic properties of the particles are measured using a vibrating sample magnetometer (VSM – Oxford VSM 1.2 H).

The glasses are prepared in desired dimension and polished in order to obtain glass thickness of around 1.5–2 mm. Optical absortion spectra of the polished glasses are characterized using UV–vis–NIR spectroscopy (Shimadzu UV–3101PC) in the wavelength range of 400–2000 nm at room temperature [2,11]. Two radiation sources are used for measurement of absorption spectra i.e. a deuterium lamp and a halogen lamp. Thermal stability of the glasses is measured using differential thermal analyzer (DTA – ParkinElmer) [2,3]. The flow of energy (heat) into or out the sample is measured as a function of temperature. The DTA measurement is cunducted in a temperature range from 50 to 700 °C with ramped temperature of 10 °C/min and alumina as reference. DTA thermograf confirms a broad endothermic and exothermic peaks related to the glass transition temperature T_g, the cristallization temperature T_c and the melting temperature T_m.

Electron spin resonance (ESR) measurements are performed using a X–Band Microwave Jeol (JES–FA100) spectrometer at room temperature and a modulation frequency of 100 kHz. The microwave frequency is 9.028 GHz. The magnetic field is scanned from 300 to 400 mT. The ESR is a powerful method for exploring spin dynamics in different bulk

magnetic material including ferro and antiferromagnet as well as spin glasses [14]. When the molecules of solid exhibit paramagnetism as a result of unpaired electron spins, transitions of spin states can be induced by applying a external magnetic field and then supplying electromagnetic energy, usually in the microwave range of frequencies. The resulting absorption spectra are described as electron spin resonance. The energy associated with the transition is expressed in terms of the applied magnetic field B, the electron spin g–factor, and the constant m_B which is called the Bohr magneton. The g–factor is value, which is given by the classical resonance condition for free electron in a magnetic field.

Results and Discussion

Properties of the particles

The LVSEM image reveals that the particles are not uniform in terms of surface morphology and size as shown in Fig. 1. Size of the pulverized particles is in nanometer to micrometer scale and some particles in nanometer scale agglomerate. Arrows indicate, the particles size is in nanometer scale.

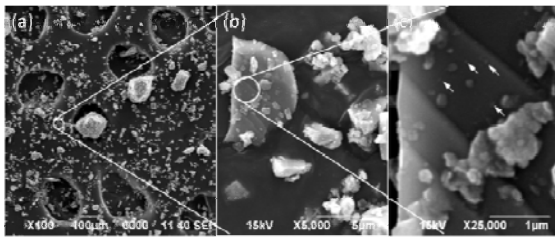

Fig. 1. LV–SEM images of the pulvervized iron sand

Fig. 2 shows XRD pattern of the particles. Almost the difraction peaks can be indexed to an inverse spinel structure of Fe_3O_4 particles, except peak at $2\theta = 33.02°$ which confirms to Fe_2O_3 particles . The strong diffraction peak at $2\theta = 35.47°$ relates to the spinel phase of Fe_3O_4 crystals [2]. Meanwhile the peaks of pulvervized iron sand at $2\theta = 27.87°$, 30.14°, 43.06°, 57.00° and 62.60° are diffraction peaks of Fe_3O_4 nanoparticles. The crystallite size is about 33–146 nm estimated using the Scherrer's formula at λ=1.54 Å

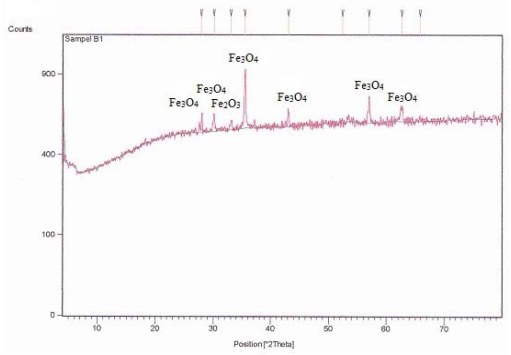

Fig. 2. XRD pattern of the pulverized iron sand

Magnetic properties of the particles are studied using VSM at room temperature and sweep width of external magnetic field from -1 to 1 T [3]. VSM yields a magnetic hysteresis curve, which confirms relationship between magnetization M (emu g^{-1}) and an external magnetic field H (T). Important parameters in determining the magnetic properties based on the hysteresis curve are saturation magnetization M_s, remanent magnetization M_r and coercivity field H_c. Measurements of magnetization versus applied external magnetic field are shown in Fig. 3. It can be seen that the hysteresis curve is very narrow with M_r = 10 emu g^{-1} and H_c = 0.02 T. The magnetization of the particles increase with increasing the applied fields and reach saturation at H_s = 0.25 T (2 x 10^5 A m^{-1}) with M_s = 55.19 emu g^{-1} (55.19 A m^2 kg^{-1}) for positive region. The susceptibility χ_m of the measured particles, i.e. 2.76 x 10^{-4} m^3 kg^{-1} is ratio between M_s and H_s related to magnetic properties [3,15].

This behavior exhibits characteristic of paramagnetic material.

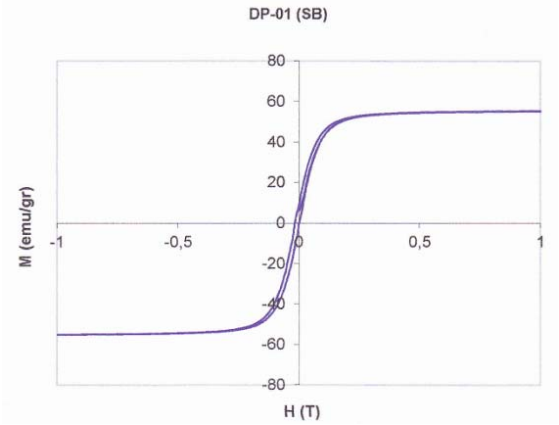

Fig. 3. M–H hysteresis curve of the pulverized iron sand particles at room temparature.

Properties of the glasses

Two different glasses are made using melt quenching technique without and with the natural Fe_3O_4 particles, hereinafter referred to as TZLF1 and TZLF2, respectively. Density (ρ) of the glasses is determined using Archimedes method [16] with toluene (99.99% pure) as an buoyant fluid at room temperature. The density of the undoped glass slighty decreases from 5.07 g cm^{-3} to 5.06 g cm^{-3} with the presence of the Fe_3O_4 concentrations. This can be understood because the molecular weight of tellurite (127.6) is much higher than iron (55.845), which substitute tellurite atoms in the glasses. The decreasing density will influence on structural compactness of the glass.

Incorporation of the particles changes color of the glass from transparent bright yelow to dominant black and non-hygroscopic. Color change is indicated, the Fe_3O_4 particles is successfully doped in the glass system leading to glass property changes [2]. The XRD spectra of the glasses are shown in Fig. 4. It can be observed that no sharp peaks are found in the spectra, only presence of a broad hunch over the region 20–35° for 2θ values, which are characteristic of amorphous state.

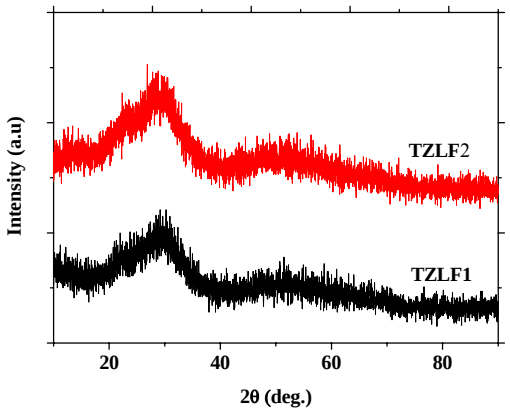

Fig. 4. XRD pattern of the glasses.

Fig. 5 shows the DTA thermograf of the glass samples. The samples exhibit a distinct endothermic peak due to glass transition and a sharp exothermic peak due to the crystallization. The TeO_2 glass containing Fe_3O_4 shows the higher glass transition temperature T_g (302 °C) than TeO_2 glass (281 °C). Increasing T_g due to endothermic indicates, the doped glass has strong bonding between their components. The bridging oxigen atoms in the glass is reduced by presence of Fe_3O_4. Fe^{+2} ions break oxigen bond and build three bonds with oxigen in the doped glass [2,3] . Fe^{2+} ions in octahedral site changed to stable Fe^{3+} ions by taking one electron from the oxigen, that occured during the quench from the liquid to the glassy state [17]. It is also occurred on the thermal stability T_c–T_g. Increasing thermal stability from 135 °C to 145 °C proved that adding Fe_3O_4 improves the glass formation ability. The other exothermic event between T_g and T_c are crystalization temperature T_c of ZnO. The melting temperature T_m of the doped glass is higher than the undoped glass.

The optical transitions and electronic band structure of materials can be studied from the optical absorption edge in UV-region [18,19]. Fig. 6 shows the absorption coefficient as function of wavelenght for the different glasses in the UV-vis-NIR optical absorption regions. It can be observed that the optical absorption edge are significantly shift toward longer wavelenght with presence of the Fe_3O_4 nanoparticles. The absorption cut-off is taken as the wavelength at which the optical absorption edge begins to increase abruptly. The cut-off wavelength increases from 400 to 1024 nm due to increasing non-bridgin oxygen in the glasses. It is well known that the excitation energy for a non-bridgin oxygen is smaller than a bridgin oxygen.

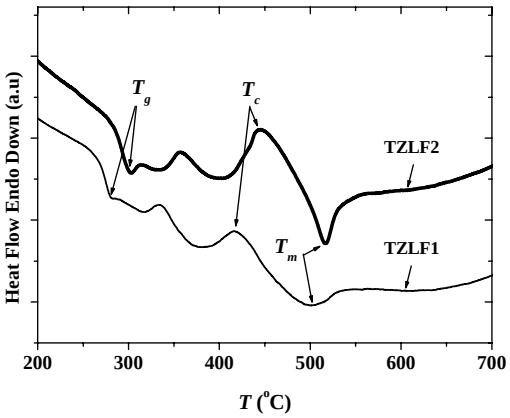

Fig. 5. DTA curves of the glasses.

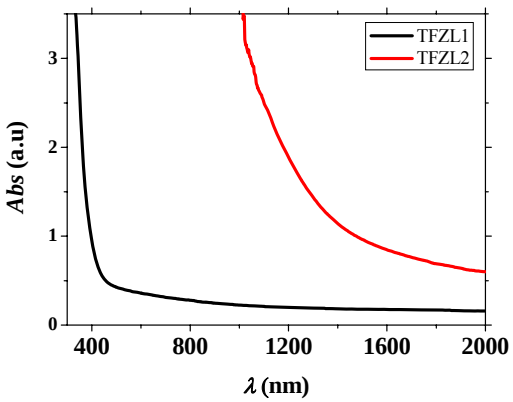

Fig. 6. Optical absorption spectra of the glasses as function of wavelenght

Based on the optical absorption edge in UV-region, the optical energy band gap of the glasses can be determined using the Davis and Mott equation [2,11,18,20]. The variation of $(\alpha h\nu)^{1/n}$ as function of photon energy in the absorption edge for n = 1/2 (direct allowed transition E_{opt}^{D}) and n = 2 (indirect allowed transition E_{opt}^{I}) are shown Fig. 7. E_{opt}^{D} and E_{opt}^{I} are determined by extrapolation of the curve's linear region to zero absorption $(\alpha h\nu)^{1/n} = 0$. It can be seen that E_{opt}^{D} and E_{opt}^{I} of the glasses significantly decreases by 1.90 eV and 1.58 eV, respectively after introducing the nanoparticles. This may be attributed by boardening valence band due to electrons of Fe atoms. It should be note that metalization in the glasses will cause the decreasing energy band gap. As consequently, the electrons only need small energy to move from the valence band to the conduction band.

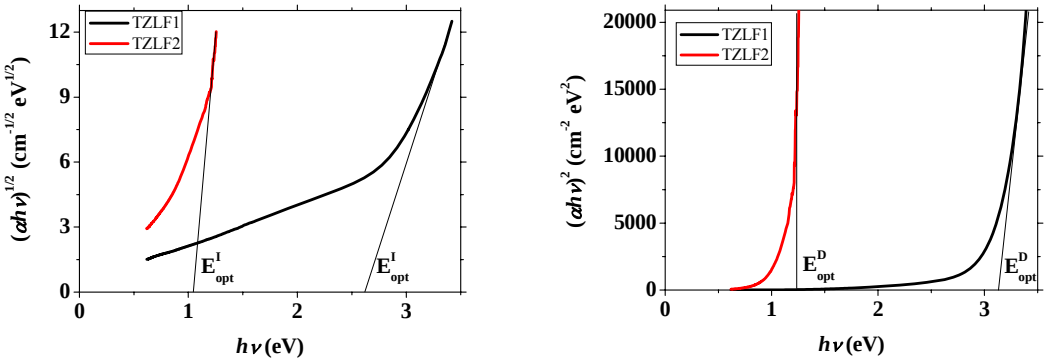

Fig. 7. The optical energy band gap for (a) indirect and (b) direct allowed transitions.

The ESR absorption spectra of the glass samples are recorded at room temperature as shown in Fig. 8. From the spectrum of undoped glass, spectrum peaks are found at g = 1.9872 (323.621 mT) and g = 1.9189 (336.195 mT). Peak *A* can be related to 2s electrons characteristic of a localized Li^+ ion. An ESR spectrum peak of the lithium lactate at g factors 2.0035 and 2.0029 has been reported [21,22]. Peak *B* confirms to 5p electrons characteristic of a localized Te^{+4} ion. Amorphous TeO_2 contains Te^{4+} cations in six-fold octahedral coordination to oxygen [23]. Accordingly to electron configuration of Te, there are two unpaired electrons in 5p block. Therefore, the combined effect of the applied field and the microwave frequency will influence their spins. The spectrum peaks indicate that spin transition occurs from -1/2 to +1/2. Meanwhile, spectrum peak due to Zn^{+2} ion can not be observed because it is an antiferromagnetic or has not unpaired electron spin in 4s block.

Addition of the natural Fe_3O_4 particles in the glass has reduced resonance amplitudo of the ESR signal. The peak due to Li^+ can be not observed anymore, whereas small peak *C* due to Te^{+4} is still appear at g = 1.9189 (336.195 mT). Loss of Li^+ signal in the doped glass can be related to an oxidation reduction process between Li^+ and Fe^{+2} because Fe^{+2} ions in octahedral site are responsible for the net magnetization related to unpaired electron spins in Fe_3O_4 specimen. Li^+ is chemically oxidized by Fe^{+2}. Meanwhile Te^{+4} is chemically reduzed by Fe^{+2}. Decreasing unpaired electrons of Te^{+4} leads to a reduction in the absorption of the magnetic field. It is proved by decreasing spectrum peak *C*. However, the doped glass exhibit paramagnetic behaviour due to presence of the unpaired electron spins in the glass.

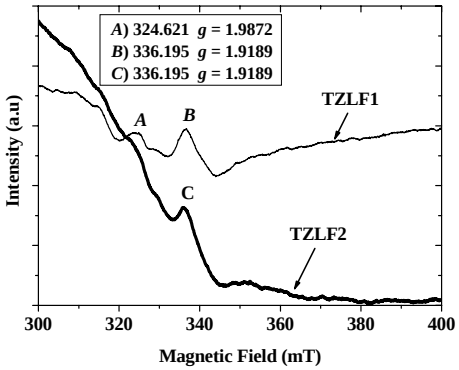

Fig. 8. ESR spectra of the glasses at room temperature.

Conclusion

A cheaper method is used in which the natural Fe_3O_4 particles are extracted from the natural iron sand. The particles doped tellurite glasses are characterized for optical and magnetic properties and role of the particles are explored. The doped glasses are found to be paramagnetic in nature and the particles strongly influence the glass formation stability, color and magneto-optic properties of these glasses. The unpaired electron spins are reduced but the ESR amplitude got enhancement. The ESR spectrum of the doped glass shows strong paramagnetic behaviour compared to the undoped glass. This observation is new and the proposed method of extracting and incorporating the particles is more economic than other existing method. The nanoparticle doped glass are promising candidate for magneto-optic devices and nanophotonics.

Acknowledgements

The authors gratefully acknowledge Universitas Jenderal Soedirman and Universiti Teknologi Malaysia for financial support of the research project.

References

[1] G. Salazar-alvarez, Synthesis , Characterisation and Applications of Iron Oxide Nanoparticles, KTH Materialvetenskap SE-100 44 Stockholm SWEDEN, 2004.
[2] W. Widanarto, M.R. Sahar, S.K. Ghoshal, R. Arifin, M.S. Rohani, K. Hamzah, J. Magn. Magn. Mater. 326 (2013) 123–128.
[3] W. Widanarto, M.R. Sahar, S.K. Ghoshal, R. Arifin, M.S. Rohani, M. Effendi, Materials Letters 108 (2013) 289–292.
[4] O. u. Rahman, S.C. Mohapatra, S. Ahmad, Mater. Chem. Phys. 132 (2012) 196–202.
[5] N.A. Zarifah, M.K. Halimah, M. Hashim, W.M. Daud, Chalcogenide Lett. 7 (2010) 565–571.
[6] A. Mekki, G.D. Khattak, L.E. Wenger, J. Non-Cryst. Solids 352 (2006) 3326–3331.
[7] N. Machida, R. Fuchida, T. Minami, Solid Stat. Lonics 35 (1989) 295–298.
[8] W.A. Dutton, W.C. Cooper, Chem. Rev. 66 (1966) 657.
[9] M. Abdel-baki, F. El-Diasty, F. Wahab, Opt. Commun. 261 (2006) 65–70.
[10] C.Z. Tan, J. Arndt, J. Magn. Magn. Mater.s 222 (1997) 391–395.
[11] W. Widanarto, M.R. Sahar, S.K. Ghoshal, R. Arifin, M.S. Rohani, K. Hamzah, M. Jandra, Mater. Chem. Phys. 138 (2013) 174–178.
[12] R.K. Singh, A. Srinivasan, J. Magn. Magn. Mater 323 (2011) 330–333.
[13] A.M. Abdel-Hameed, M.A. Marzouk, A.E. Abdel-Ghany, J. Non-Cryst. Solids 357 (2011) 3888–3896.
[14] S. Mukherjee, H.D. Yang, A.K. Pal, S. Majumdar, J. Non-Cryst. Solids 324 (2012) 1690–1697.
[15] Callister, Material Science and Engineering an Introduction, 6th ed., John Wiley & Sons, (Asia) Pte. Ltd., 2003.
[16] Sulhadi, Structural and Optical Properties Studies of Erbium Doped Tellurite Glasses, Universiti Teknologi Malaysia, 2007.
[17] M.D. Dyar, M.T. Naney, S.E. Swanson, American Mineralogist 72 (1987) 792–800.
[18] G. Kiliç, E. Aral, G.U. J. Sci. 22 (2009) 129–139.
[19] I. Jlassi, H. Elhouichet, S. Hraiech, M. Ferid, J. Lumin. 132 (2012) 832–840.
[20] G. Prakash, D. Rao, A. Bhatnagar, Solid State Communications 119 (2001) 39–44.

[21] G.M. Hassan, M. Ikeya, S. Toyoda, Appl. Radiat. Isot. 49 (1998) 823–828.
[22] M. Ikeya, G.M. Hassan, H. Sasaoka, Y. Kinoshita, S. Takaki, C. Yamanaka, Appl. Radiat. Isot. 52 (2000) 1209–1215.
[23] M.S. Malik, C.A. Hogarth, K.A.K. Lott, J. Mater. Sci. 25 (1990) 1909–1912.